24th ABCM International Congress of Mechanical Engineering
December 3-8, 2017, Curitiba, PR, Brazil

COBEM-2017-1170
EXPERIMENTAL RESEARCH OF CAPILLARY STRUCTURE TECHNOLOGIES FOR HEAT PIPES

Larissa Krambeck[1]
Guilherme A. Bartmeyer[1]
Davi Fusão[1]
Paulo H. D. Santos[2]
Thiago Antonini Alves[1]
Federal University of Technology – Paraná, [1]Ponta Grossa/PR, [2]Curitiba/PR, Brazil
larikrambeck@hotmail.com, gabartmeyer@hotmail.com, davi@utfpr.edu.br, psantos@utfpr.edu.br, thiagoaalves@utfpr.edu.br

Abstract. *This paper presents an experimental research of three different capillary structure technologies of heat pipes for the application in the thermal management of electronic packaging. The first capillary structure is axial grooves manufactured by wire electrical discharge machining (wire-EDM). The sintering process with copper powder produced the second heat pipe. Finally, a hybrid heat pipe was manufactured by the combination of the two previous processes. The heat pipes were produced by a copper tube with an outer diameter of 9.45 mm and length of 200 mm. The working fluid used was deionized water. The heat pipes were tested horizontally to increasing heat loads varying from 5 to 35 W. The experimental results showed that all capillary structures of the heat pipes worked successfully, so the used manufacturing methods are suitable. Nonetheless, the hybrid heat pipe is the best, due to the lowest thermal resistance presented.*

Keywords: *heat pipe, axial grooves, wire-EDM, sintered metal powder, experimental.*

1. INTRODUCTION

The thermal management of electronic packaging has become a key technique in many products. Due to the innovation of modern electronic technology, the thermal systems miniaturization and the consequent rapid increase in power density of advanced microprocessors and electronic components created a significant demand for achieving high heat dissipation rates (Nishida *et al.*, 2014). In most cases, such high heat fluxes cannot be easily dissipated using existing cooling techniques, directly affecting the performance, cost, and reliability of devices. Heat pipes can be a good alternative for such applications (Ghajar and Darabi, 2014). According to Faghri (2014), heat pipes are highly effective passive devices for transmitting heat at high rates over considerable distances with small temperature decrease, flexibility, simple construction, and easy control with no external pumping power.

The heat pipes operate according to the following principle (Groll and Rösler, 1992): in the evaporator region, heat is transferred to the heat pipe, vaporizing the working fluid contained inside this region. The steam generated is moved, due to the pressure and density differences, to the condenser where heat transported is rejected to the cold source. In the heat rejection process, the steam condenses, and the condensate returns back to the evaporator closing the cycle. The adiabatic region may have variable dimensions or be absent and it is located between the evaporator and the condenser being insulated from the external environment. The working fluid returns from the condenser to the evaporator due to capillary pumping effect. A schematic diagram of the operating principle of heat pipes is presented in Fig. 1. More details on the principle of the heat pipes can be found in Chi (1976), Peterson (1994), and Reay *et al*. (2014).

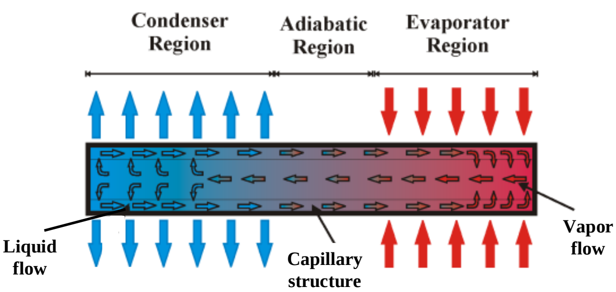

Figure 1. Sketch of the operating principle of a heat pipe

A heat pipe consists essentially of three components: an involucre, a working fluid, and a capillary structure. The most common capillary structures are screens, sintered metals, and axial grooves (Peterson, 1994). There are several types of grooves cross sections inside copper heat pipes, such as triangular, rectangular, trapezoidal, and inverse trapezoidal, resulting in different heat transfer performances (Nishida *et al.*, 2015). The way producing ideal inner grooves is the main problem with the heat pipes (Reay *et al*., 2014). The conventional manufacturing methods, such as milling and broaching, are expensive and can be difficult for a small production (Li *et al*., 2008). The sintered metal wicks are manufactured by packing tiny metal particles between the inner heat pipe wall and a mandrel in powder form (Tang *et al.*, 2013). A hybrid structure is the improvement of the heat pipe performance by the conciliation of two common capillary structures (Paiva and Mantelli, 2015).

In this research, three capillary structure technologies of heat pipes for application in the thermal management of electronic packaging is experimental researched. A grooved heat pipe has semicircular axial grooves manufactured using wire electrical discharge machining (wire-EDM). A sintered heat pipe was produced with spherical copper powder and a temporary mandrel, which placed powder in the annulus region. And, a hybrid heat pipe was manufactured by the combination of two previous methods, wire-EDM, and sintering.

2. EXPERIMENTAL PROCEDURE

The methodology for manufacture (cleaning, assembly, tightness test, evacuation procedure, and filling with the working fluid); test; and analysis of the heat pipes were developed based on Nishida (2016), Krambeck (2016), and Santos *et al.* (2017).

2.1 Characteristics of Developed Heat Pipes

The heat pipes were produced by copper tubes (ASTM B-75 Alloy 122) with an outer diameter of 9.45 mm and length of 200 mm. The heat pipes have an evaporator region of 80 mm in length, an adiabatic region of 20 mm in length, and a condensation region of 100 mm in length. The working fluid used was deionized water with filling ratios based on the best performance of each capillary structure. Table 1 presents the main characteristics of heat pipes analysed in this research.

Table 1. Main characteristics of heat pipes.

Characteristics	**Heat Pipe**		
	Grooved	**Sintered**	**Hybrid**
Inner diameter [mm]	7.00	7.75	7.00
Outer diameter [mm]	9.45	9.45	9.45
Evaporator [mm]	80	80	80
Adiabatic section [mm]	20	20	20
Condenser [mm]	100	100	100
Working fluid	Deionized water	Deionized water	Deionized water
Filling ratio [%]	60	100	100
Volume of working fluid [mL]	1.60	2.80	2.41
Capillary Structure	21 Axial microgrooves	Sintered copper powder	21 Axial microgrooves with sintered copper powder
Manufacturing Method	Wire-EDM	Sintering	Wire-EDM with sintering

The grooved heat pipe had 21 microgrooves made by the wire electrical discharge machining or wire-EDM. The Figure 2 presents the axial microgrooves details with an average diameter of 220 µm by a micro-scale image. The image was obtained by Backscattered Electron Detector (BSD) for Scanning Electron Microscope (SEM). More details about this heat pipe can be found in Nishida (2016) and Krambeck *et al.* (2017).

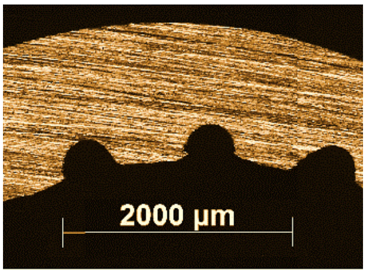

Figure 2. Capillary structure of the Grooved Heat Pipe – SEM micrograph

The sintered heat pipe was produced by the sintering process with a copper powder and a temporary mandrel. The average diameter of the copper powder particle is 10.9 μm. The porous structure manufactured has a thickness of 1.6 mm (Fig. 3a). The micro-scale image of the capillary structure of sintered copper powder is presented in Fig. 3b.

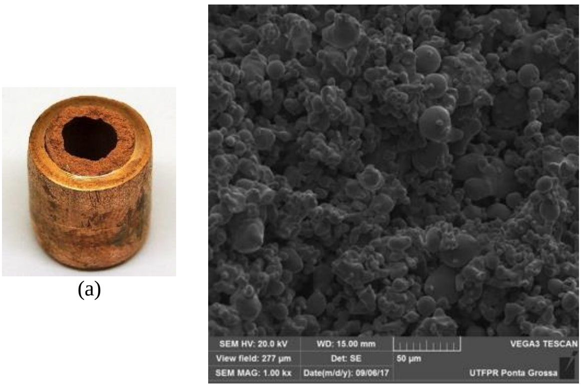

(a) (b)

Figure 3. Capillary structure of the Sintered Heat Pipe

The hybrid heat pipe with the same number axial microgrooves made by wire-EDM, 21, has been sintered with copper powder and the mandrel used in the sintered heat pipe construction. Due to the smaller inner diameter, the thickness of the sintered structure was approximately 1.3 mm. Figure 4 presents the combination of microgrooves and the sintered copper powder that compose the capillary structure.

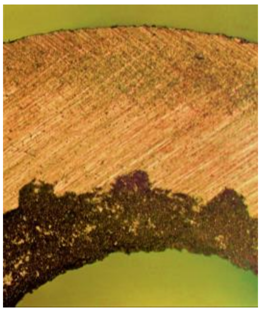

Figure 4. Capillary structure of the Hybrid Heat Pipe

2.2 Experimental Apparatus

The experimental apparatus used for the experimental tests, shown in Fig. 5, is composed of a power supply unit (*Agilent™* U8002A), a data logger (*Agilent™* 34970A with 20 channels), a *Dell™* desktop,), an uninterruptible power supply (*NHS*™), a universal support, and an *Ultrar™* fan.

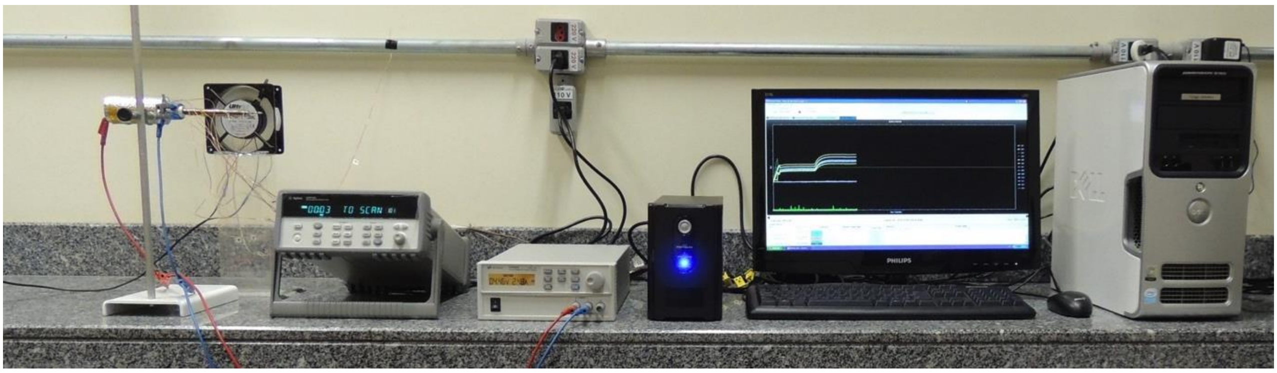

Figure 5. Experimental apparatus

For the evaluation of the thermal performance of the heat pipes, K-type thermocouples *Omega*™ were used. They were fixed on the outer surface of heat pipe by a thermosensitive adhesive strip *Kapton*™. As shown in Fig. 6, there were three thermocouples in the evaporator ($T_{evap,1}$, $T_{evap,2}$, and $T_{evap,3}$), one thermocouple in the adiabatic section (T_{adiab}) e four thermocouples in the condenser ($T_{cond,1}$, $T_{cond,2}$, , $T_{cond,3}$, and $T_{cond,4}$) in heat pipes.

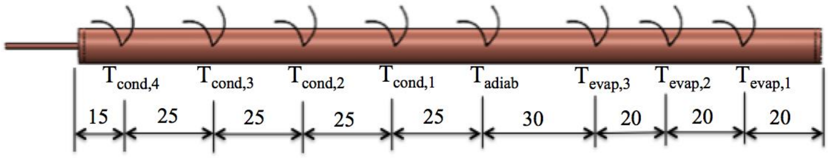

Figure 6. Thermocouples positions [mm]

The heating system of the evaporator was conducted by power dissipation in a nickel-chromium alloy power strip resistor *Omega*™ with 0.1 mm of thickness and 3.5 mm in width. To ensure that the generated heat by Joule effect was transmitted to the evaporator, an aeronautic thermal insulation and a layer of polyethylene were installed in this region. A fiberglass tape was used in adiabatic section as heat insulation between the support and the heat pipe. The cooling system using air forced convection consisted of a fan in the condenser region.

2.3 Experimental Procedure

To ensure the best results and the repeatability of experimental tests, the ambient temperature was maintained at 20.0 °C ± 1.0 °C by the thermal conditioning system *York™*. The heat pipe was carefully fixed to the universal support with bracket in the adiabatic region at the horizontal position. The fan was turned on, positioned correctly in the condenser region and set at a speed of 5.0 m/s with a combined error of ± 0.2 m/s. The data acquisition system was turned on, and the temperatures measured by the K-type thermocouples. The power supply unit was turned on and adjusted to the dissipation power desired. The initial load was 5W and, after approximately 15 minutes, when the thermocouples showed stationary values. The load increment was made until the maximum average temperature of the heat pipe reached the critical temperature (150 ºC), where the melting of the materials could happen. Data was acquired every five seconds, recorded on the laptop by the software *Agilent™ Benchlink Data Logger* 3. The experimental uncertainties are associated to the K-type thermocouples, the data logger, and the power supply unit. The experimental temperature uncertainty is estimated to be approximately ± 1.27 °C and a thermal load was ± 1%. For the uncertainties determination, the error propagation method described by Holman (2011) was used.

2.4 Data Reduction

The performance of the capillary structures was analyzed and compared with the operation temperature and the thermal resistance. The operation temperature analyzed was the temperature from the adiabatic region. The total thermal resistance, R_{th}, of a heat pipe can be defined as the difficulty of the device to carry heat. The higher the thermal resistance, the greater the difficulty is in transporting heat from the system (Bergman *et al*., 2011). The total thermal resistance can be calculated by

$$R_{th} = \frac{\Delta T}{q} = \frac{\left(T_{evap} - T_{cond}\right)}{q}, \tag{1}$$

where, q is the heat transfer capability of the device, T_{evap} and T_{cond} are the average wall temperature of the evaporator and the condenser, respectively.

3. RESULTS AND DISCUSSION

The experimental results regarding the thermal behavior of the heat pipes with different capillary structure technologies operating in the horizontal position are presented. The experimental tests were repeated three times and the errors were compared taking into account the difference between the mean values were less than 0.5 °C. The tests were performed at increasing heat loads 5 W, ranging from 5 up to 35 W. Figure 7 shows the temperature distributions as a function of time for the heat pipes with different capillary structures (grooved, sintered, and hybrid). For all the capillary structure technologies, the maximum dissipated power was 35 W. The hybrid and the sintered heat pipe obtained the behavior more isothermal than the grooved heat pipe.

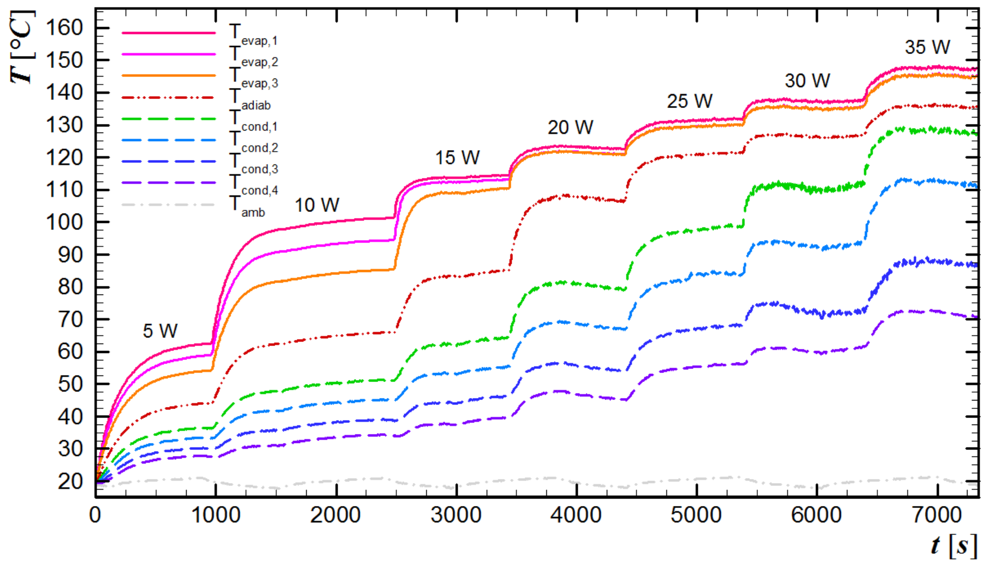

(a) Grooved

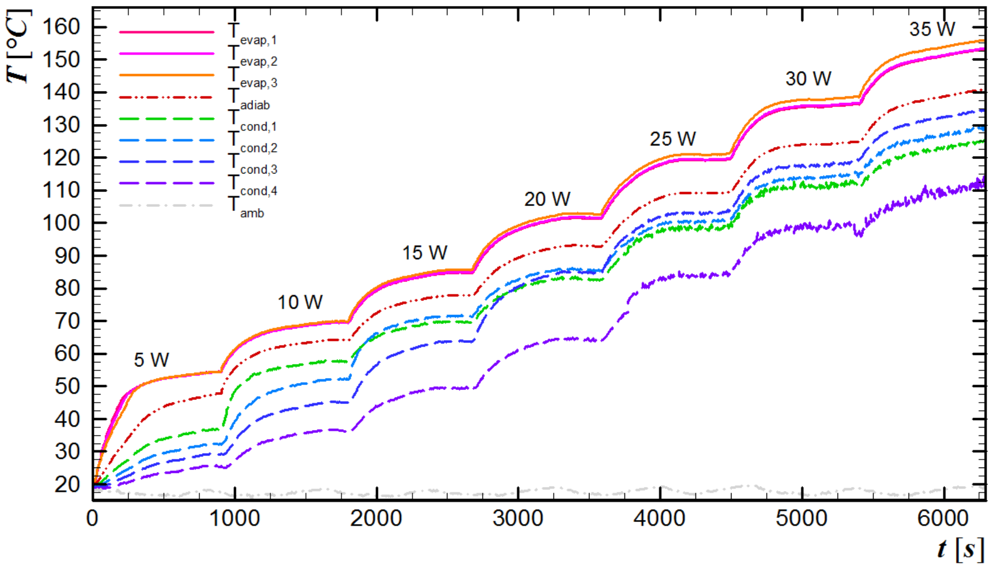

(b) Sintered

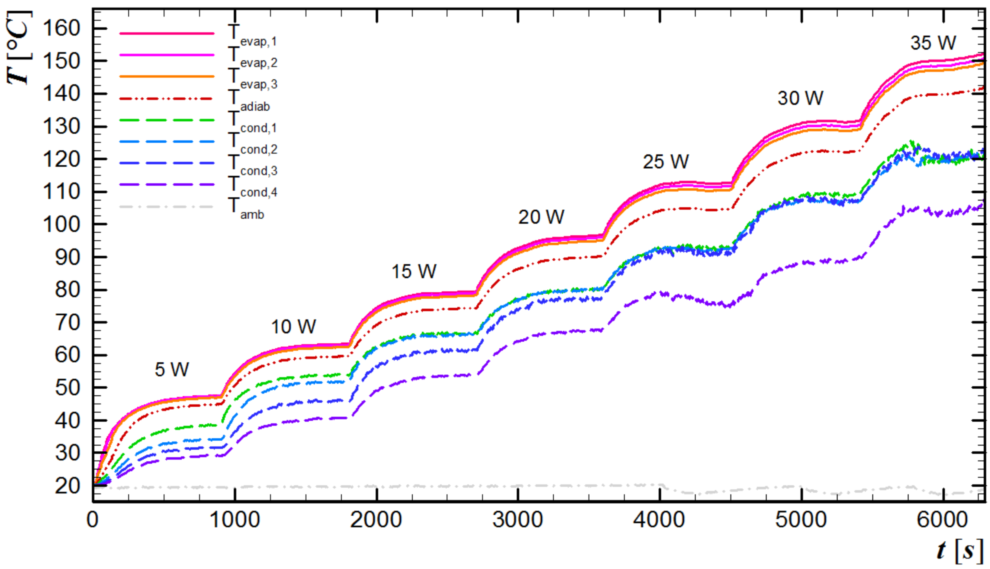

(c) Hybrid

Figure 7. Temperature distribution *vs* time of heat pipes

The operation temperature in function of the heat load is shown in Fig. 8. Figure 9 illustrates the behavior of the thermal resistance as a function of power dissipation considering the three different capillary structures. The operation temperature increases with the rise of the heat load. The heat pipes' thermal resistance decrease with the increasing heat dissipation in the evaporator.

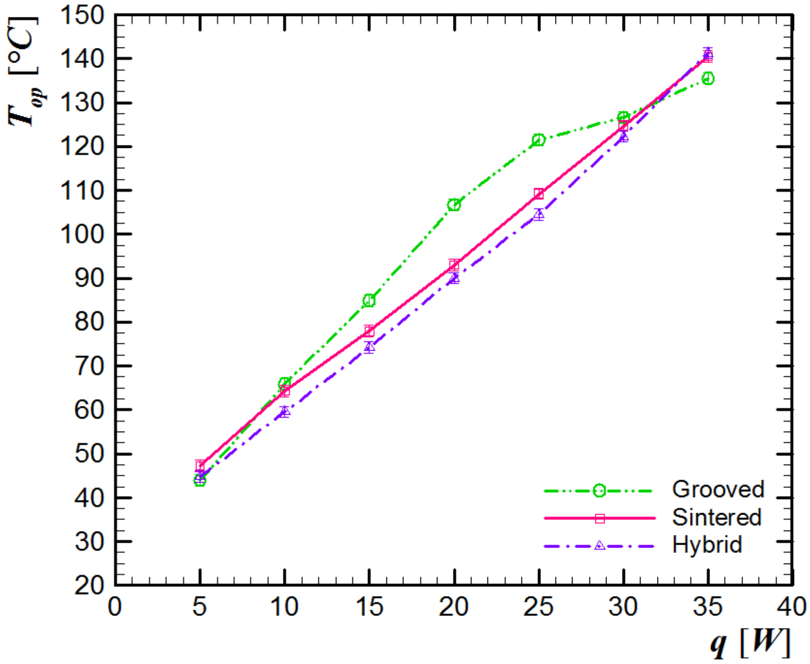

Figure 8. Operation temperature *versus* heat load of different capillary structures

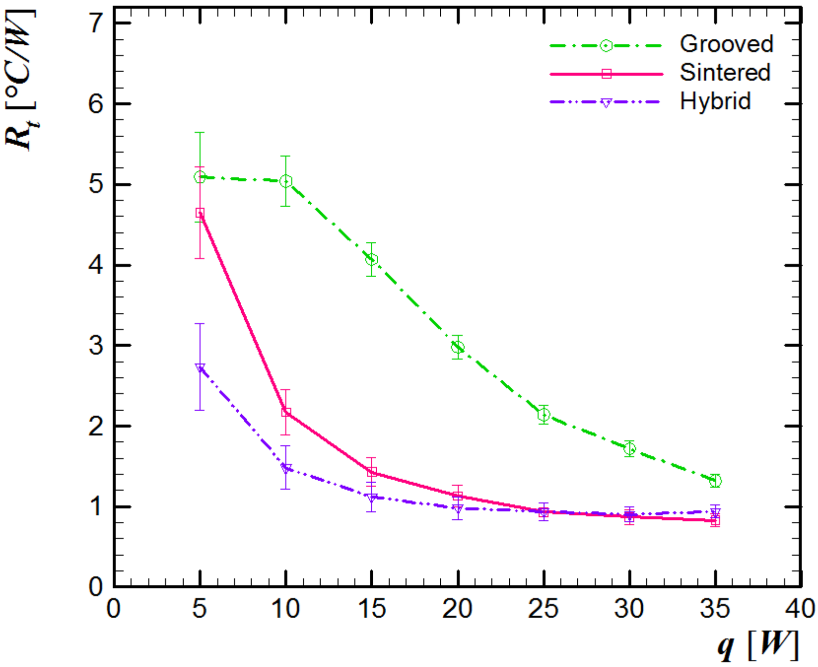

Figure 9. Thermal resistance *versus* heat load of different capillary structure technologies

All the heat pipes worked successfully, since the capillary structures provided to the heat pipes the operation in a higher load and lower thermal resistance. Thus, the results were satisfactory since the intention of these tests was to evaluate the efficiency of the manufacturing methods of the capillary structures. So, the manufacturing methods are suitable. Also, the hybrid is the best capillary structure technology, due to the lowest thermal resistance and a slightly lower operating temperature than the other heat pipes.

4. CONCLUSIONS

This paper presented an experimental research of three heat pipes with different capillary structure technologies for the application in the thermal management of electronic packaging. The studied heat pipes were grooved, sintered metal powder, and hybrid. The heat pipes were tested horizontally and used deionized water as working fluid. As a result of the study, all the heat pipes worked successfully, so the used manufacturing methods are suitable. Nonetheless, the hybrid heat pipe is the best, due to the lowest thermal resistance presented.

5. ACKNOWLEDGEMENTS

Acknowledgments are provided to the Capes, the CNPq, the PROPPG/UTFPR, the DIRPPG/UTFPR, the PPGEM/ UTFPR/Ponta Grossa, and the DAMEC/UTFPR/Ponta Grossa.

6. REFERENCES

Bergman, T.L., Lavine, A.S., Incropera, F.P. & DeWitt, D.P., *Fundamentals of Heat and Mass Transfer*, John Wiley & Sons., New York, USA, 2011.

Chi, S.W., 1976. *Heat Pipe Theory and Practice: A Sourcebook.* Hemisphere Publishing Corporation, Washington, USA.

Ghajar, M., Darabi, J., 2014. “Evaporative Heat Transfer Analysis of a Micro Loop Heat Pipe with Rectangular Grooves”. *International Journal of Thermal Sciences*, Vol. 79, pp. 51-59.

Groll, M., Rösler, S., 1992. “Operation Principles and Performance of Heat Pipes and Closed Two-Phase Thermosyphons”. *Journal of Non-Equilibrium Thermodynamics*, Vol. 17, pp. 091-151.

Faghri, A., 2014. “Heat Pipes: Review, Opportunities and Challenges”. *Frontiers in Heat Pipes*, Vol. 5, pp 01-48.

Holman, J. P., 2011. *Experimental Methods for Engineers.* McGraw-Hill, New York, USA.

Krambeck, L., 2016. *Experimental investigation of wire mesh thermal performance in heat pipes.* Graduation work, Federal University of Technology – Paraná, Ponta Grossa, Brazil (in Portuguese).

Krambeck, L., Nishida, F.B., Santos, P.H.D. & Antonini Alves, T., Heat pipe with axial microgrooves fabricated by wire electrical discharge machining (wire-EDM), *9th World Conference on Experimental Heat Transfer, Fluid Mechanics and Thermodynamics*, Brazil, 2017.

Li, Y., Xiao, H., Lian, B., Tang, Y., Zeng, Z., 2008. “Forming method of axial grooves inside copper heat pipe”. *Transactions of Nonferrous Metals Society of China*, Vol. 18, pp. 1229–1233.

Mantelli, M.B.H., *Tubos de Calor e Termossifões*, Notas de Aula, Departamento de Engenharia Mecânica, Universidade Federal de Santa Catarina, Florianópolis, SC, Brasil, 2015.

Nishida, F.B., 2016. *Development of heat pipes with microgrooves fabricated by wire electrical discharge machining*. M.Sc. dissertation, Federal University of Technology – Paraná, Ponta Grossa, Brazil (in Portuguese).

Nishida, F.B., Marquardt, L.S., Borges, V.Y.S., Santos, P.H.D, Antonini Alves, T., 2015. “Development of a copper heat pipe with axial grooves manufactured using wire electrical discharge machining (wire-EDM)”. *Advanced Materials Research (Online)*, Vol. 1120-1121, pp. 1325-1329.

Nishida, F.B., Tadano, Y.S., Antonini Alves, T., 2014. “Conjugate Forced Convection-Conduction Heat Transfer in Channel Flow using Different Cooling Fluids”. In *Proceedings of the 15th International Heat Transfer Conference* - IHTC15-9594. Kyoto, Japan.

Paiva, K.V., Mantelli, M.B.H., 2015. “Wire-plate and sintered hybrid heat pipes: model and experimental”. *International Journal of Thermal Sciences*, Vol. 93, pp. 36–51.

Peterson, G.P., 1994. *An Introduction to Heat Pipes: Modeling, Testing and Applications, (Thermal Management of Microelectronic and Electronic System Series).* Wiley-Interscience, New York, USA.

Reay, D.A., Kew, P.A., McGlen, R.J., 2014. *Heat Pipe: Theory, Design and Applications*. Butterworth-Heinemann, Amsterdam, NED.

Santos, P.H.D., Reis, L.S., Marquardt, L.S., Vicente, K.A.T., Antonini Alves, T., 2017. “Modeling and Experimental Tests of a Copper Thermosyphon”. *Acta Scientiarum. Technology*, Vol. 39, pp. 59-68.

Tang, Y., Deng, D., Huang, G., Wan, Z., Lu, L., 2013. “Effect of fabrication parameters on capillary performance of composite wicks for two-phase heat transfer devices”. *Energy Conversion and Management*, Vol. 66, pp. 66-76.

7. RESPONSIBILITY NOTICE

The authors are the only responsible for the printed material included in this paper.